Applied Catalysis A: General 471 (2014) 136–141

Contents lists available at ScienceDirect

Applied Catalysis A: General

journal homepage: www.elsevier.com/locate/apcata

A novel fluidized-bed-optical-fibers photocatalytic reactor (FBOFPR) and its performance

Rongshu Zhu[a,b,c], Sainan Che[a,b,c], Xianbo Liu[a,b,c], Songxue Lin[a,b,c], Guilin Xu[a,b,c], Feng Ouyang[a,b,c,*]

[a] *Environmental Science and Engineering Research Center Harbin Institute of Technology Shenzhen Graduate School, Shenzhen 518055, Guangdong, PR China*
[b] *Shenzhen Key Laboratory of Water Resource Utilization and Environmental Pollution Control, Shenzhen 518055, Guangdong, PR China*
[c] *Public Platform for Technological Service in Urban Waste Reuse and Energy Regeneration, Shenzhen 518055, Guangdong, PR China*

ARTICLE INFO

Article history:
Received 27 July 2013
Received in revised form
24 November 2013
Accepted 30 November 2013
Available online 7 December 2013

Keywords:
Fluidized-bed-optical-fibers photocatalytic reactor
TiO_2
TCE
Apparent photon quantum efficiency
Turnover frequency

ABSTRACT

The key in designing a photocatalytic reactor lies in resolving the problems of mass transfer, light transmission and light scattering. Especially, the light scattering of catalyst is very acute, which makes the accurate quantification of light irradiation difficult. In this study, a novel fluidized-bed-optical-fibers photocatalytic reactor (FBOFPR) with easy quantification of light irradiation was designed by combining fluidized-bed photocatalytic reactor with optical-fiber light source that its optical fibers were fixed by an aluminum fixed jacket for UV total reflection, and its performance was tested by using trichloroethylene (TCE) as a target pollutant. The results show that, under the condition of water vapor content at 0.25%, oxygen content at 20.8%, initial concentration of TCE at 303.32 ppm, input light amount at $3.07 \times 10^{17}\ s^{-1}$ and residence time at 1.6 s, the apparent photon quantum efficiency is 26.31%, the turnover frequency is 12.44 μmol/(g TiO_2 min) and the removal efficiency is 86.66%. Compared with the conventional flat plate fluidized-bed photocatalytic reactor, FBOFPR exhibits many advantages in the aspect of effective use of photon, sufficient exertion of catalyst activity, effective removal of TCE and easy quantification of light irradiation.

1. Introduction

The photocatalytic reaction occurs on the light irradiated surface of photocatalyst, which means that a reactant must be in contact with the light irradiated surface of the photocatalyst to complete a photocatalytic reaction. This feature determines that the conventional fixed-bed photocatalytic reactor has no high photocatalytic efficiency due to the limitation of mass transport and light transmission during the process of reaction. The fluidized-bed photocatalytic reactor has high photocatalytic efficiency due to its highly efficient mass transfer and favorable light irradiation. However, the conventional fluidized-bed photocatalytic reactor generally exists the problems that interior light source occupies most of the volume of the reactor [1] or outer light source decreases light utilization efficiency [2]. In addition, the accurate quantification of light irradiation is difficult in these reactors [3].

Optical fiber has a capacity to transmit light. Using the side of optical fiber to supply the light to the surface of photocatalyst was first proposed by Ollis and Marinangeli [4,5]. Hofstadler et al. [6] designed the TiO_2-coated quartz optical fiber reactor (OFR) and proved the feasibility through photocatalytic degradation of 4-CP. After that, many groups [7–15] used optical fibers to supply light for photocatalytic reactor. However, the light intensity from the side of optical fiber decreases exponentially with the increase of the fibers length [12] and whether the light can refract to the surface of TiO_2 is affected by coating technology [10].

The optical fibers can not only achieve long distance transmission of the light but also realize arbitrary distribution of the light. Using the end of optical fibers to supply light for photocatalytic reactor, it can irradiate the light directly on TiO_2 surface for reaction as well as distribute the light uniformly, which will overcome the shortage of using the side of optical fiber to supply light. In addition, the output of light irradiation from the end of optical fiber is easy to quantify and the aluminum fixed jacket of optical fibers for UV total reflection can avoid the loss of scattering of light. However, it is little reported that combining fluidized-bed photocatalytic reactor with the end of optical fibers to supply light.

In this study, a fluidized-bed-optical-fibers photocatalytic reactor (FBOFPR) was designed by using the aluminum fixed jacket of

---

* Corresponding author at: Environmental Science and Engineering Research Center Harbin Institute of Technology Shenzhen Graduate School, Shenzhen 518055, Guangdong, PR China. Tel.: +86 755 26033472; fax: +86 755 26033472.
E-mail address: ouyangfh@hit.edu.cn (F. Ouyang).

0926-860X/$ – see front matter © 2013 Elsevier B.V. All rights reserved.
http://dx.doi.org/10.1016/j.apcata.2013.11.044

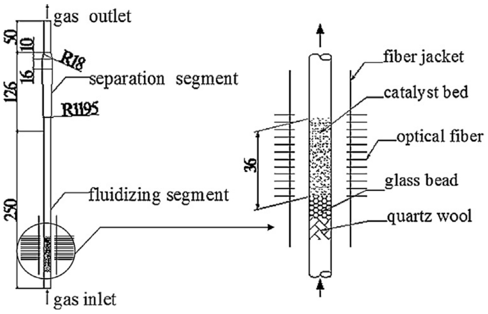

Fig. 1. Schematic diagram of FBOFPR.

optical fibers for UV total reflection to avoid the loss of scattering of light, using the end of optical fibers to supply light and combining the fluidized-bed photocatalytic technique. And its performances were studied by using TCE as removal object.

2. FBOFPR

Fig. 1 shows the schematic diagram of FBOFPR. The photocatalytic reactor contains fluidized-bed, fixed jacket of optical fibers and light source to optical fibers. The fluidized-bed is composed of gas inlet segment, fluidizing segment, separation segment and gas outlet segment. Each segment is made of quartz glass (Jinda Quartz Glass Company, Jinzhou China, UV light transmittance is more than 98%) except that the gas inlet segment is stainless steel. The parameters of the fluidized-bed are listed in Table 1. The fixed jacket of optical fibers is columniform and its material is UV total reflective aluminum plate. The diameter of the columniform fixed jackets is 34 mm and their thickness is 1 mm. The circumferential surface of the fixed jackets is fixed 8 optical fibers equidistantly and the longitudinal space of the fibers is 3.4 mm. In order to contrast to the aluminum fixed jacket for UV total reflection, the fixed jacket was also made by rubber sheet. The light source to optical fibers is provided by UV spot light source (L8333-01, Hamamatsu, Japan) and transported through the optical fiber (A4094-01, Hamamatsu, Japan) to fluidized-bed. The UV lamp (L8251, Hamamatsu, Japan) can give wavelength range of the light in 280–400 nm after filtered by optical filter (A7028-03, Hamamatsu, Japan) and its main wavelength is 365 nm.

3. Experimental

3.1. Measurement of light irradiation

The amount of light emitted from the optical fibers was measured by using the method of potassium ferrioxalate actinometry [16,17]. The process included five steps: (1) The preparation of photolysis liquid: dissolved 0.7369 g $K_3Fe(C_2O_4)_3{\cdot}3H_2O$ into deionized water, added 0.675 mL fuming sulfuric acid, then diluted to 250 mL, achieved 0.006 mol/L $K_3Fe(C_2O_4)_3$ solution. (2) The preparation of buffer solution: dissolved 80 g ammonium acetate into 100 mL glacial acetic acid, then diluted to 200 mL. (3) The preparation of chromogenic agent: dissolved 0.5 g phenanthroline into deionized water, droped muriatic acid as an auxiliary agent, then diluted to 100 mL. (4) The measurement of the amount of light emitted from the optical fibers: took 20 mL photolysis liquid, located at 10 mm away from the end of the optical fibers, irradiated 1 min, 5 min, 10 min, 20 min, respectively, then got 1 mL photolysis liquid to colorimetric tube with stopper, added 5 mL buffer solution, 2 mL chromogenic agent and diluted to 50 mL, maintained 5–10 min, the light absorption of Fe^{2+} was measured at 510 nm, where the concentration of Fe^{2+} in photolysis liquid could be obtained from the standard curve. Plotting with time as an abscissa and concentration of Fe^{2+} as an ordinate, the slope $d[Fe^{2+}]/dt$ obtained. (5) The calculation of the amount of light emitted from the optical fibers: the light absorption of photolysis liquid per volume could be calculated through Eq. (1), where I is the amount of light irradiation, N_A is Avogadro's constant and is 6.022×10^{23}, V_p is the volume of photolysis liquid and is 0.02 L, Φ is luminous flux and is 1.26 at the wavelength of 365 nm. According to this measurement and calculation method, the total amount of light irradiation (I_{total}) in present reactor is $3.07 \times 10^{17}\ s^{-1}$.

$$I = N_A \times V_p \times \frac{d[Fe^{2+}]/dt}{\Phi} \quad (1)$$

Table 1
Parameters of fluidized-bed.

Parameters	Size (mm)
Outer diameter of the gas inlet segment	2
Inner diameter of the fluidizing segment	10
Height of fluidizing segment	250
Curvature radius of separating segment (down)	1195
Height of separating segment (down)	100
Inner diameter of separating segment (middle)	16
Height of separating segment (middle)	16
Curvature radius of separating segment (up)	18
Height of separating segment (up)	10
Inner diameter of the gas outlet segment	10
Height of the gas outlet segment	50

3.2. Preparation of catalyst

The photocatalyst used in the experiment was prepared through direct coating method [18]. Weighed a certain amount of TiO_2 nanoparticles (Degussa P25, ca. 75% anatase and 25% rutile, average particle size, ca. 21 nm, BET area, ca. $50 \pm 15\ m^2\ g^{-1}$), added to a certain amount of deionized water, oscillated for 0.5 h by ultrasonic and so as to form uniform TiO_2 suspensions, and adjusted its pH to 5.5 with dilute ammonia. Weighed SiO_2 (Qingdao Haiyang Chemical Co., Ltd., 0.125–0.425 mm, $460\ m^2\ g^{-1}$) accordance with the mass ratio at 10% between TiO_2 and TiO_2/SiO_2, poured the SiO_2 into the TiO_2 suspension and ultrasound for 3 h. After placed for 24 h at room temperature and dried for 12 h at 110 °C, calcined for 3 h at 200 °C using tube furnace. After sieving the catalyst, selected the desired particles for experiment.

3.3. Testing the performance of the reactor

Used glass beads of diameter of 0.250–0.425 mm as gas distribution plate. Put quartz wool about 10 mm high under the glass beads to support the glass beads and the catalysts to prevent them leaking to the gas line.

The reaction gas was composed of TCE, O_2, water vapor and N_2. N_2 acted as balance gas. N_2 and O_2 were provided by gas cylinder. TCE and water vapor were prepared by bubbling method [19]. After the reaction gas was mixed in mixing tube, the mixture gas flowed into the photocatalytic reactor at a flow rate of 106 mL/min. Weighed 1.0 g catalyst (contained 0.1 g TiO_2) and placed in the reaction tube, and the height of the fluidized bed was 36 mm after uniformly fluidizing (the reaction residence time of 1.6 s). After reached gas–solid adsorption equilibrium (identified as 5 h by equilibrium experiment), turned on the light and began the degradation experiments. The concentration of TCE was measured on line by gas chromatograph (SP-6890, Rainbow Chemical Instrument Co., Ltd., China) equipped with capillary column (50 m × 0.25 mm × 0.5 μm) and FID detector. The concentration of CO and CO_2 were measured on line by gas chromatograph (GC-112A, Precision and Scientific

Instrument Co., Ltd., China) equipped with column (Propark-Q, 80–100 mesh, 3 mm × 0.5 mm × 2.5 m) and FID detector.

The performance of the FBOFPR was evaluated by three parameters: apparent photon quantum efficiency Y (%), turnover frequency f (μmol/(g TiO_2 min)) and removal efficiency η (%).

3.3.1. Apparent photon quantum efficiency (Y)

Y is used to evaluate the light utilization efficiency of the reactor, which is defined as the percentage between the photons for the photocatalytic reaction and the total number of input photons, also called quantum yield [20]. According to the measured irradiation of UV light emitted from the end of the optical fiber to calculate the total number of input photons unit time into the photocatalytic reactor, which assumes that the input photons are absorbed completely. Because the valence state of carbon element in the organic compound is zero, it requires four photons to generate +4 valence state of CO_2 and two photons to generate +2 valence state of CO. Therefore, Y can be obtained through the ratio between the photons absorbed by CO_2 and CO generated per unit time and the amount of the light irradiation, and the formula for Y can be written as Eq. (2) [21–23]. Where V_{CO_2} and V_{CO} are the generated volume fraction of CO_2 and CO, respectively, in the steady process and their units are ppm, Q is the flow rate of the reaction gas and is 106 mL/min, V_m is the molar volume of gas and is approximates at 22.4 L/mol.

$$Y = \frac{(2V_{CO} + 4V_{CO_2}) \times Q \times N_A \times 10^{-7}}{60 \times V_m \times I_{total}} \tag{2}$$

3.3.2. Turnover frequency (f)

f is defined as unit mass of TiO_2 within unit time to remove the amount of contaminants. The formula for f can be written as Eq. (3) and its unit is μmol/(g TiO_2 min), where m is the mass of TiO_2 and is calculated at 0.1 g.

$$f = \frac{(V_{CO_2} + V_{CO}) \times Q \times 10^{-3}}{2 \times V_m \times m} \tag{3}$$

3.3.3. Removal efficiency (η)

η is used to evaluate the degradation efficiency of organic compounds by the photocatalytic reactor. It is calculated through the ratio between the generation of CO_2 and CO and the corresponding concentration of the initial total organic carbon. The formula for η can be written as Eq. (4), where V_{TCE} is the initial volume fraction of TCE and its unit is ppm.

$$\eta = \frac{(V_{CO_2} + V\mathrm{CO}) \times 10^2}{2V_{TCE}} \tag{4}$$

4. Results and discussion

Fig. 2 shows the curve of direct photolysis of TCE. From Fig. 2, it can be seen that about 10.76% of the TCE was degraded directly after turned on the light. This phenomenon is similar to that reported by many literatures [24–27]. Because the generation of CO and CO_2 was not be detected, indicating the direct photolysis of TCE was not completely degraded into CO_2 and CO, the decreasing of TCE concentration was attributed to the partial oxidation of TCE [25,26]. In this study, the final products of CO_2 and CO were used to calculate the evaluation parameters. Therefore, the direct photolysis almost has no effect on the results of the evaluation.

Fig. 2 also shows the curve of photocatalytic degradation of TCE and the generation curves of CO and CO_2 on TiO_2/SiO_2. Comparing the photolysis curve of TCE with the generation curves of CO and CO_2, it can be seen that TCE can be almost completely degraded into CO and CO_2. Many researches on the mechanism of the photocatalytic degradation of TCE have been done [25,27–30] and the degradation process includes: TCE → dichloro acetyl chloride (DCAC) → CO, CO_2, H_2O, HCl and phosgene. The results that reported by Fan and Yates [29] and Amama et al. [30] show that the addition of H_2O can promote DCAC and phosgene be converted to CO_2. Thus, it is possible that the organic carbon of TCE can be totally degraded into CO and CO_2 in present of water vapor.

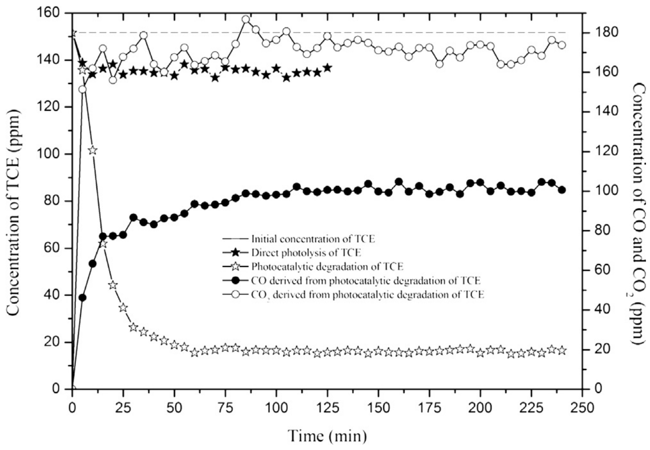

Fig. 2. The degradation of TCE. Reaction conditions: initial concentration of TCE: 151.66 ppm; water vapor content: 0.25%; oxygen content: 20.8%; total amount of the light irradiation: $3.07 \times 10^{17}\ s^{-1}$; material of fixed jacket: rubber.

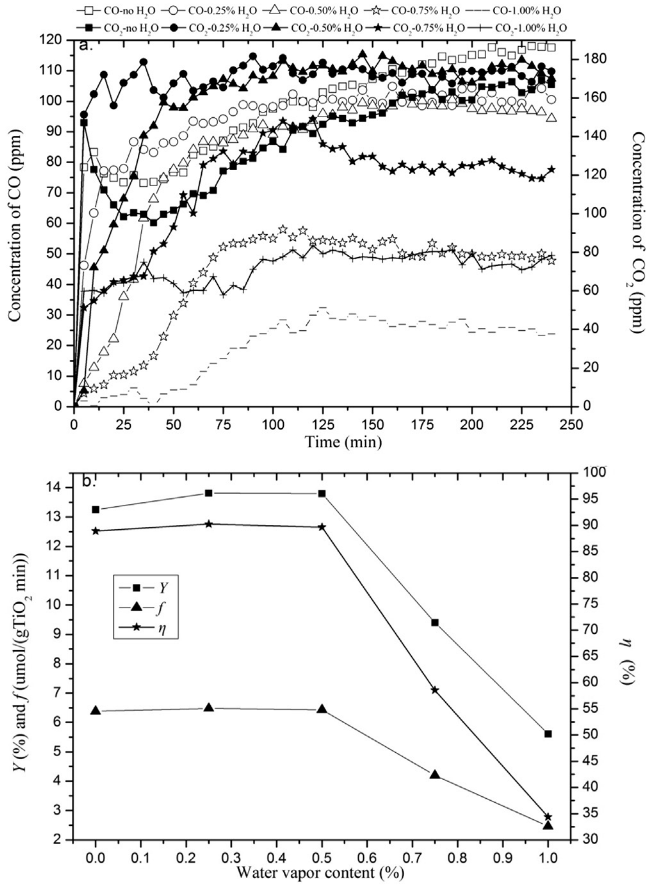

Fig. 3. The effects of water vapor content on the degradation of TCE: (a) the generation curves of CO_2 and CO; (b) the corresponding results of Y, f and η. Reaction conditions: initial concentration of TCE: 151.66 ppm; oxygen content: 20.8%; total amount of light irradiation: $3.07 \times 10^{17}\ s^{-1}$; material of fixed jacket: rubber.

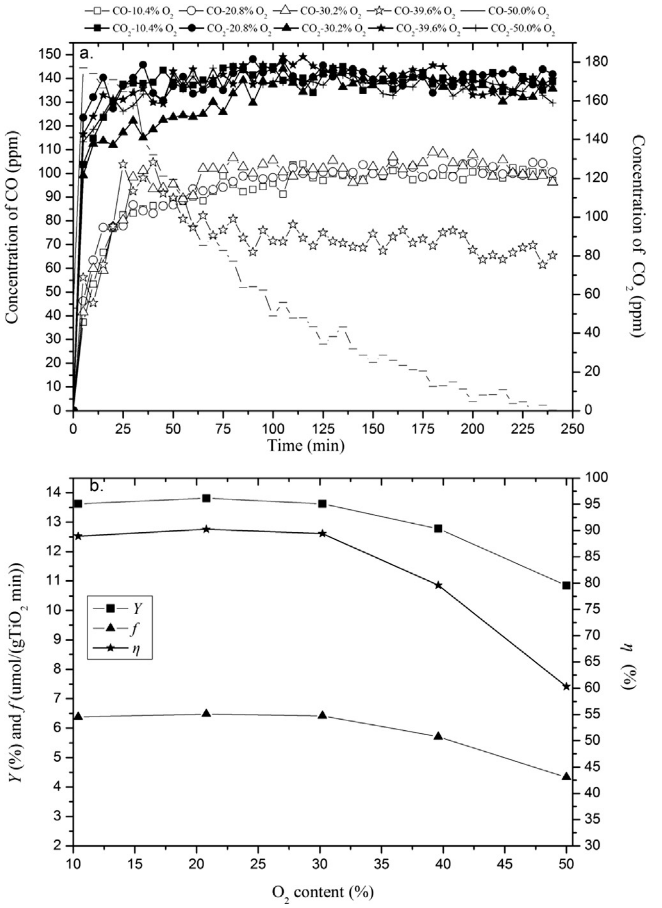

Fig. 4. The effects of oxygen content on the degradation of TCE: (a) the generation curves of CO_2 and CO; (b) the corresponding results of *Y*, *f* and *η*. Reaction conditions: initial concentration of TCE: 151.66 ppm; water vapor content: 0.25%; total amount of light irradiation: 3.07×10^{17} s^{-1}; material of fixed jacket: rubber.

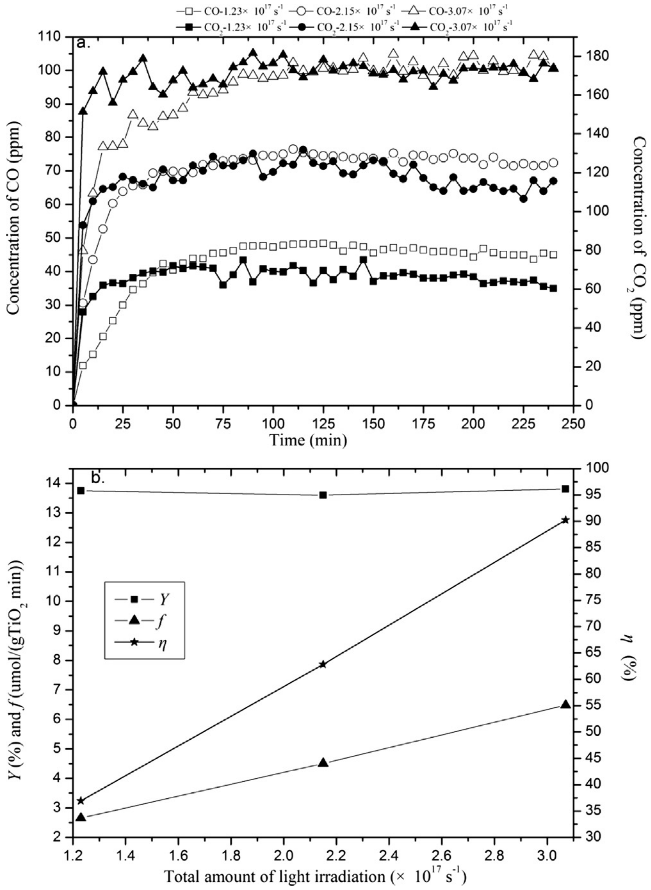

Fig. 5. The effects of total amount of light irradiation on the degradation of TCE: (a) the generation curves of CO_2 and CO; (b) the corresponding results of *Y*, *f* and *η*. Reaction conditions: initial concentration of TCE: 151.66 ppm; water vapor content: 0.25%; oxygen content: 20.8%; material of fixed jacket: rubber.

Fig. 3a shows the generation curves of CO_2 and CO in the process of photocatalytic degradation of TCE under different water vapor content and the corresponding results of *Y*, *f*, *η* are shown in Fig. 3b. As can be seen from the data in Fig. 3b, a small amount of water vapor can enhance the degradation of TCE and the removal efficiency of TCE decreases with the increase of the water vapor content when the content of water vapor increases to a certain extent. The phenomena that lower water vapor content almost does not affect the degradation activity of TCE and higher water vapor content inhibits the degradation of TCE are consistent with many literatures [2,31–35], which is because excessive water molecules will compete active sites of catalyst surface with TCE or intermediate species. However, the phenomenon that small amount of water vapor can enhance the degradation of TCE is not consistent with these literatures [2,31–35]. This discrepancy may arise from our data processing. From the generation curves of CO and CO_2 under the condition of no water vapor in Fig. 3a, we can see that the curves first decrease fast with the time of photocatalytic reaction increasing, then start to rise gradually after 25 min and do not achieve the desired steady degradation until 240 min. In order to facilitate data comparison, the data under the condition of no water vapor was analyzed by same processing as other data, which may lead to a slightly lower result than that obtained in actual degradation. For the results that the generation of CO and CO_2 decreases firstly and then increase slowly with the time increase (as shown in Fig. 3a), it is because the degradation rate of DCAC is slower than that of TCE by approximate one order [27]. That is the slowly degradation of DCAC leads to the generation of CO and CO_2 not achieving the expected steady degradation until 240 min (as shown in Fig. 3a).

Fig. 4a shows the generation curves of CO_2 and CO in the process of photocatalytic degradation of TCE under different O_2 content and the corresponding results of *Y*, *f*, *η* are shown in Fig. 4b. As can be seen from Fig. 4b, it has little effect on the degradation of TCE when the content of oxygen changes in the range of 10.4–30.2% and the degradation of the oxygen content at 20.8% is slightly better than the degradation at other oxygen content, which is consistent with the results that reported by Wang et al. [34]. Wang et al. [34] studied the effects of oxygen content on the degradation of TCE in the range of 0–20% and found the degradation rate of TCE did not change significantly when oxygen content was higher than 10%. During the oxygen content raising from 30.2% to 50.0%, the efficiency of degradation decreases. This phenomenon is similar to that reported by Ou and Lo [27] and Demeestere et al. [36]. They thought that is mainly because the excess of oxygen adsorbs on the catalyst surface and competes the active sites with TCE. It is worth noting that the decrease of TCE degradation is directly related to the production of CO (as shown in Fig. 4, the generation of CO_2 is the same, whereas the generation of CO decreases obviously under the oxygen content of 39.4% and 50.0%) and its mechanism needs to be further researched.

Fig. 5a shows the generation curves of CO_2 and CO in the process of photocatalytic degradation of TCE under different total amount of light irradiation and the corresponding results of *Y*, *f*, *η* are shown in Fig. 5b. From the data in Fig. 5b, it can be clearly seen that *η* and *f* increases as the total amount of light irradiation increases. This is

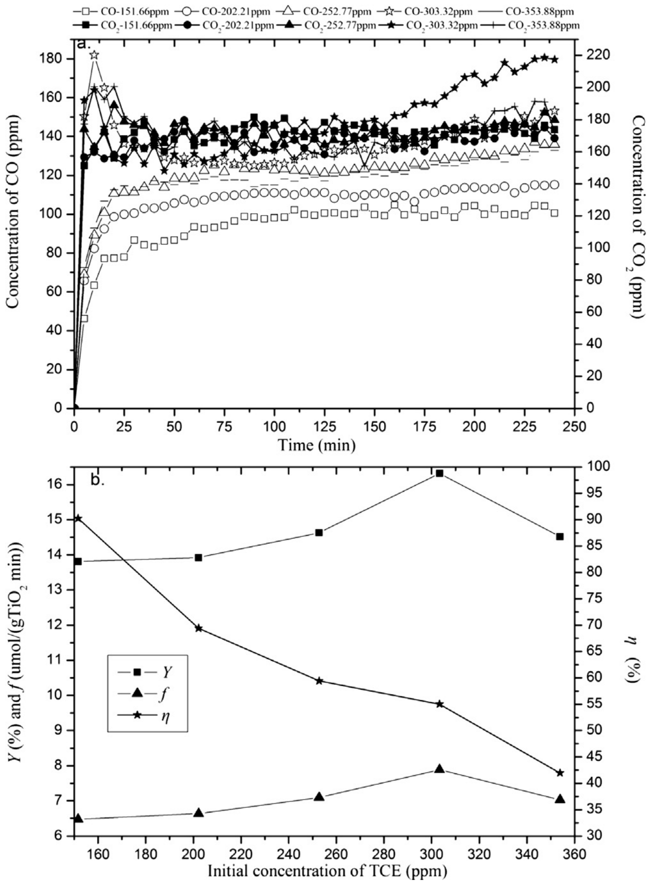

Fig. 6. The effects of initial concentration of TCE on the degradation of TCE: (a) the generation curves of CO_2 and CO; (b) the corresponding results of Y, f and η. Reaction conditions: water vapor content: 0.25%; oxygen content: 20.8%; total amount of light irradiation: 3.07×10^{17} s^{-1}; material of fixed jacket: rubber.

because the greater amount of light irradiation can provide more photons, the more active sites are produced and the better degradation of TCE is achieved [33,34]. These results are similar to that reported by Dibble and Raupp [2]. It should be noted that Y did not change significantly with the increasing of the total amount of light irradiation. Wang et al. [33,34] reported that the quantum efficiency decreased with the increasing of light intensity, which is not consistent with our results. For the difference from the result that reported by Wang et al. [33,34], it may be because the performance of our reactor is limited by the mass transfer of TCE under this condition. Thus we further researched the effects of initial concentration of TCE.

Fig. 6a shows the generation curves of CO_2 and CO in the process of photocatalytic degradation of TCE under different initial concentration of TCE and the corresponding results of Y, f, η are shown in Fig. 6b. From the data in Fig. 6b, it can be seen that, within the range of 150–350 ppm, the η decreases, while Y and f firstly increases and then decreases with the increasing of initial concentration of TCE. For η decreases with the increasing of the initial concentration of TCE, it is mainly because the quantity of active site is a certain number, which results in that the degradation of TCE cannot increase in proportion to the increasing of initial concentration of TCE. For Y and f increase with the increasing of the initial concentration of TCE, it is agreement with the prediction under different total amount of light irradiation, which Y and f can be improved if the mass transfer is not limited. For the Y and f further decrease with the initial concentration increasing, based on the similar shape of the generation curves of CO_2 and CO under the concentration of TCE at 303.32 ppm in Fig. 6a and under anhydrous conditions in Fig. 3a (the generation curves of CO and CO_2 first decreases sharply then increases slowly with extent of photocatalytic reaction time), it suggests that the degradation is limited by water vapor content. Although the addition of H_2O can promote DCAC and phosgene be converted to CO_2 [29,30], the degradation of high concentration of TCE forms a large accumulation of DCAC and its concentration exceeds a proportion of H_2O. The work of optimization of H_2O content at high concentration of TCE will be further carried out.

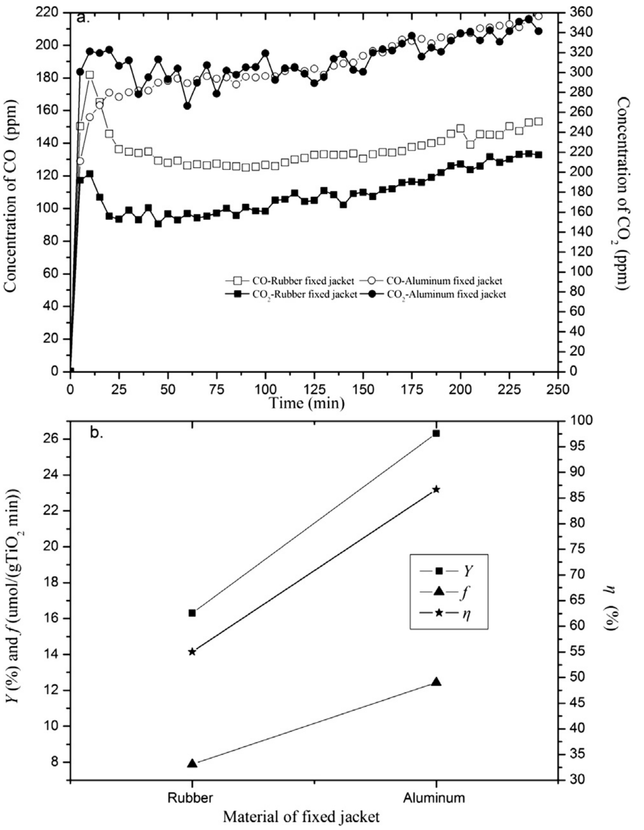

Fig. 7. The effects of material of fixed jacket on the degradation of TCE: (a) the generation curves of CO_2 and CO; (b) the corresponding results of Y, f and η. Reaction conditions: initial concentration of TCE: 151.66 ppm; water vapor content: 0.25%; oxygen content: 20.8%; total amount of light irradiation: 3.07×10^{17} s^{-1}.

Fig. 7a shows the generation curves of CO_2 and CO in the process of photocatalytic degradation of TCE with different materials of fixed jacket of optical fibers and the corresponding results of Y, f, η are shown in Fig. 7b. From Fig. 7, it can clearly be seen that the degradation of TCE significantly improves with the aluminum fixed jacket. Compared with the result that using rubber fixed jacket, η increases by 31.66%, Y increases by 9.99% and f increases by 4.55 μmol/(g iO_2 min). This is mainly because the aluminum fixed jacket reflects the ultraviolet light to avoid the loss of scattering of light and thus improves the utilization of light.

Dibble and Raupp [2] obtained the highest turnover frequency of TCE was 2 μmol/(g TiO_2 min) and the highest quantum efficiency was 13% in flat plate fluidized-bed reactor. Furthermore, the catalyst reversibly deactivated once the initial concentration of TCE was higher than 10 ppm. Compared with the performance of Dibble's reactor [2], FBOFPR improves the turnover frequency of the catalyst by about 6 times and the apparent photon quantum efficiency by about 2 times under steady state. In addition, no catalyst deactivation occurred when initial concentration was higher than 300 ppm.

From all above, combining the fluidized-bed photocatalytic reactor with the light source from optical fiber that was fixed by the aluminum fixed jacket for UV total reflection to design an easy quantification fluidized-bed-optical-fibers photocatalytic reactor, it exhibits great advantage in the effective use of photon, the sufficient exertion of catalyst activity, the effective removal of TCE and the easy quantification of light irradiation.

5. Conclusion

FBOFPR with easy quantification of light irradiation was designed by combining the fluidized-bed photocatalytic reactor with optical-fiber light source that the optical fibers were fixed by the aluminum fixed jacket for UV total reflection. Under the condition of water vapor content at 0.25%, oxygen content at 20.8%, initial concentration of TCE at 303.32 ppm, total amount of light irradiation at 3.07×10^{17} s^{-1} and residence time at 1.6 s, the apparent photon quantum efficiency is 26.31%, the turnover frequency is 12.44 μmol/(g TiO_2 min) and the removal efficiency is 86.66%. Compared with the conventional flat plate fluidized-bed photocatalytic reactor, FBOFPR exhibits many advantages in the aspect of effective use of photon, sufficient exertion of catalyst activity, effective removal of TCE and easy quantification of light irradiation.

Acknowledgments

All the authors gratefully acknowledge support from the Special Fund for the Development of Strategic and New Industry in Shenzhen (No. JCYJ20120613114951217), the National Natural Science Foundation of China (No. 20907012) and the Fund for the Research and Development of Science and Technology in Shenzhen (No. CXZZ20130516145955144).

References

[1] R.L. Pozzo, J.L. Giombi, M.A. Baltanas, A.E. Cassano, Catal. Today 62 (2000) 175–187.
[2] L.A. Dibble, G.B. Raupp, Environ. Sci. Technol. 26 (1992) 492–495.
[3] M.I. Cabrera, O.M. Alfano, A.E. Cassano, Ind. Eng. Chem. Res. 33 (1994) 3031–3042.
[4] D.F. Ollis, R.E. Marinangeli, AIChE J. 23 (1977) 415–426.
[5] D.F. Ollis, R.E. Marinangeli, AIChE J. 26 (1980) 1000–1008.
[6] K. Hofstadler, R. Bauer, S. Novalic, G. Heisler, Environ. Sci. Technol. 28 (1994) 670–674.
[7] N.J. Peill, M.R. Hoffmann, Environ. Sci. Technol. 29 (1995) 2974–2981.
[8] A. Sirisuk, C.G. Hill, M.A. Anderson, Catal. Today 54 (1999) 159–164.
[9] R.D. Sun, A. Nakajima, I. Watanabe, T. Watanabe, K. Hashimoto, J. Photochem. Photobiol. A 136 (2000) 111–116.
[10] W. Choi, J.Y. Ko, H. Park, J.S. Chung, Appl. Catal. B 31 (2001) 209–220.
[11] J. Hyunku, J. Heerok, J. Myungseok, Sol. Energy Mater. Sol. Cells 79 (2003) 93–101.
[12] W. Wang, Y. Ku, Chemosphere 50 (2003) 999–1006.
[13] P. Du, J.T. Carneiro, J.A. Moulijn, G. Mul, Appl. Catal. A 334 (2008) 119–128.
[14] A. Danion, J. Disdier, C. Guillard, F. Abdelmalek, N. Jaffrezic-Renault, Int. J. Appl. Electrom. 23 (2006) 187–201.
[15] D.D. Li, L.L. Wang, G.J. Zhang, Opt. Commun. 286 (2013) 182–186.
[16] C.G. Hatchard, C.A. Parker, Math. Phys. Sci. 235 (1956) 518–536.
[17] J. Lee, J. Kim, W. Choi, Environ. Sci. Technol. 41 (2007) 5433–5438.
[18] N.J. Peill, M.R. Hoffmann, Environ. Sci. Technol. 30 (1996) 2806–2812.
[19] X.Q. Shan, T.B. Wang, Z.M. Ni, Fresen. Z. Anal. Chem. 326 (1987) 419–424.
[20] L.Z. Sun, J.R. Bolton, J. Phys. Chem. C 100 (1996) 4127–4134.
[21] M. Schiavello, V. Augugliaro, L. Palmisano, J. Catal. 127 (1991) 332–341.
[22] O.M. Alfano, M.I. Cabrera, A.E. Cassano, Chem. Eng. Sci. 49 (1994) 5327–5346.
[23] C.S. Mei, S.H. Zhong, Acta Chim. Sinica-Chin. Ed. 63 (2005) 1789–1794.
[24] M. Zhang, T. An, X. Hu, Acta Sci. Circumst. 25 (2005) 259–263.
[25] C.R. Jiang, C.L. Zheng, X.Y. Li, L.Y. Wan, W.S. Zhang, G.H. Chen, Chem. J. Chin. Univ. 30 (2009) 539–543.
[26] M.R. Nimlos, W.A. Jacoby, D.M. Blake, T.A. Milne, Environ. Sci. Technol. 27 (1993) 732–740.
[27] H.H. Ou, S.L. Lo, J. Hazard. Mater. 146 (2007) 302–308.
[28] K.H. Wang, J.M. Jehng, Y.H. Hsieh, C.Y. Chang, J. Hazard. Mater B90 (2002) 63–75.
[29] J.F. Fan, J.T. Yates, J. Am. Chem. Soc. 118 (1996) 4686–4692.
[30] P.B. Amama, K. Itoh, M. Murabayashi, J. Mol. Catal. A 217 (2004) 109–115.
[31] L.A. Dibble, G.B. Raupp, Catal. Lett. 4 (1990) 345–354.
[32] K.H. Wang, H.H. Tsai, Y.H. Hsieh, Appl. Catal. B 17 (1998) 313–320.
[33] K.H. Wang, Y.H. Hsieh, Environ. Int. 24 (1998) 267–274.
[34] K.H. Wang, H.H. Tsai, Y.H. Hsieh, Chemosphere 36 (1998) 2763–2773.
[35] H. Márta, D. András, Appl. Catal. A: Gen. 271 (2004) 177–184.
[36] K. Demeestere, J. Dewulf, H. Van Langenhove, Crit. Rev. Environ. Sci. Technol. 37 (2007) 489–538.